Magnetic Control of Translational and Torsional Motions of Suspended Loads

Panagiota Atzampou, Peter Meijers(✉), Apostolos Tsouvalas, and Andrei Metrikine

Delft University of Technology, Stevinweg 1, 2628CN Delft, The Netherlands
p.c.meijers@tudelft.nl

Abstract. The present study introduces a coupled contactless control approach for managing both translational and torsional motions of a suspended load. This method utilizes magnet-to-magnet interactions between two pairs of magnetic dipoles, with translational motion controlled by adjusting the polarity and intensity of the electromagnetic actuator, and torsional motion regulated through the orientation of the external magnetic field. The results demonstrate effective motion dissipation in response to external excitations and non-trivial initial conditions. Key control parameters include the initial distance between interacting magnets and the ability of translational control to counteract the attractive forces generated by torsional torque. The proposed magnetic control method presents a promising foundation for non-contact position control in offshore wind turbine installations.

Keywords: Magnetic control · Magnetic dipole · PID control · Active vibration control · Offshore wind turbine installation

1 Introduction

The ever-increasing energy demands have driven the growth in wind turbine generator (WTG) size and capacity, necessitating installations in deeper waters. These installations are conducted by floating vessels operating on dynamic positioning. Despite their greater lifting capacities, these vessels are highly susceptible to wave-induced oscillations in the crane-payload system. Controlling the motion of suspended loads is critical for operational safety and efficiency. Various motion compensation techniques have been employed over the years. While various compensation methods, such as active tugger lines [8], gripper frames [5], and crane motion compensators are available [6,7], they rely on mechanical attachments and human intervention. This fact, coupled with the small error tolerances required and the limited workability windows available for the operations, further highlights the paucity of research for a non-contact motion compensation technique for WTG installation.

Á. Cunha and E. Caetano (Eds.): EVACES 2025, LNCE 676, pp. 37–45, 2025.
https://doi.org/10.1007/978-3-031-96114-4_5

The proposed technique is based on the magnet-to-magnet interaction between the component and electromagnetic actuators, involving both attractive and repulsive forces. To demonstrate the concept, a small-scale pendulum analogue is modelled and analysed, investigating the controllability of a two-degree-of-freedom dynamical system. The system's vibrational modes, which pertain to the translational and torsional modes of motion of the payload, significantly affect the accuracy of the WTG assembly. The aim of the control is to attenuate the effects of a prescribed pivot point motion and initial conditions and to maintain a desired fixed position.

This paper first introduces the dynamical system, emphasizing the magnetic coupling. Then, the control design is presented with a focus on stability requirements. Finally, the controlled response of the system is demonstrated for selected initial conditions and external disturbances. Special attention is given to the efficiency of the combined control and its impact on the system's dynamical behaviour, including the nonlinear coupling effects from magnetic interactions.

2 Methodology

2.1 Governing Equations of a Controlled Planar Torsional Magnetic Pendulum

A small-scale simple pendulum analogue with length ℓ is augmented with a cylindrical mass M that is free to rotate around its shaft (longitudinal axis). The coupled model is illustrated in Fig. 1, while the dimensions and properties of the system are given by Table 1. In principle, the set-up integrates the two SDOF systems reported in previous work [1,2]. The control design requires the action of two separate electromagnetic actuators: one controlling the rotation of the mass in xz-plane (translation) and the other in xy-plane (torsional rotation). In the envisioned practical application, the suspended mass is an elongated cylindrical structure (e.g., an OWT monopile foundation). Such geometry allows for an advantageous placement of contactless control points at different heights along its length on one side of the load, ideally on the floating vessel's deck. For simplicity, in this study of the combined control, two permanent magnets are attached to opposite sides of the cylindrical mass, represented by magnetic dipoles.

Table 1. Set-up parameters of the dynamic 2DOF system.

M [kg]	ℓ [m]	R [mm]	τ [mm]	k_s [N mm/°]	I_z [kg mm^2]	f_n [Hz]
0.2	1.0	20.0	2.0	50	36.2	[0.5, 4.2]

Potential interactions between the magnetic fields of the mounted dipoles or direct interference from one actuator affecting the field of the other as experienced by the targeted fixed magnet are neglected in the current analysis, as

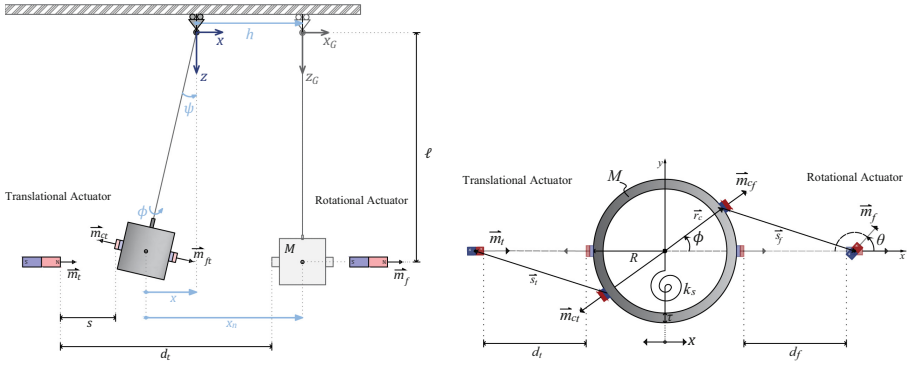

(a) xz-plane (b) xy-plane

Fig. 1. Schematic of the pendulum set-up for the combined control of its translational and torsional degree of freedom.

such interactions would not occur in practical applications, due to adequate separation distance between the control points and respective actuators (along the structure's z-axis). Note that the suspended load is adequately small to be considered a point mass in the derivations. The motion of the pivot is described by $h = A_h \sin(\Omega t)$.

Two electromagnetic actuators are placed at a fixed distance on either side of the load, d_t for the translational and d_f for the torsional controller. I_z is the moment of inertia of the mass around the z-axis, and k_s is analogous to the stiffness provided by the suspension cable and experienced by the mass rotating in this direction (Fig. 1b).

The equations of motion of this two-degree-system are the following [3,4]:

$$M\ell^2\ddot{\psi} + Mg\ell\psi = -M\ddot{h}\ell + T_t \tag{1a}$$

$$I_z\ddot{\phi} + k_s\phi = T_f, \tag{1b}$$

where the external magnetic torques are equal to

$$T_t = -\frac{\partial W_m}{\partial \psi} \tag{2a}$$

$$T_f = -\frac{\partial W_m}{\partial \phi} \tag{2b}$$

W_m is the contribution of the pairs of interacting magnetic dipoles to the potential energy of the system and is equal to

$$W_m = -\sum \vec{m}_{cn} \cdot \vec{B}_n, \tag{3}$$

in which $\vec{B}_n$ is the magnetic field exerted by the EM ($\vec{m}_n$) to the location of the respective PM on the cylindrical point mass ($\vec{m}_{cn}$), where the general subscript

notation n is either t for the translational or f for the torsional control. The magnetic field vector $\vec{B}_n$ reads

$$\vec{B}_n = -\frac{\mu_0}{4\pi}\vec{\nabla}\frac{\vec{m}_n \cdot \vec{s}_n}{s_n^3}, \tag{4}$$

in which, $\vec{s}_n$ denotes the vector representing the separation distance between the two dipoles (see Fig. 1b). The magnitude of s_n is calculated by the following norm:

$$s_n = ||\vec{P}_n - \vec{P}_{cn}||, \tag{5}$$

with the coordinates of the magnetic dipoles given by

$$\vec{P}_n = \begin{bmatrix} i_n(R+d_n) \\ 0 \\ \ell \end{bmatrix} \text{ and } \vec{P}_{cn} = \begin{bmatrix} \ell\sin(\psi)+h \\ 0 \\ \ell\cos(\psi) \end{bmatrix} + i_n \begin{bmatrix} R\sin(\phi) \\ R\cos(\phi) \\ 0 \end{bmatrix}, \tag{6}$$

with $i_n = -1$ or $+1$ for the translational and the rotational control, respectively.

Referring to Fig. 1b, the vectors representing the four magnetic dipole moments are given by

$$\vec{m}_t = M_t \begin{bmatrix} 1 \\ 0 \\ 0 \end{bmatrix} \text{ and } \vec{m}_{ct} = -M_{ct} \begin{bmatrix} \cos(\phi) \\ \sin(\phi) \\ 0 \end{bmatrix} \tag{7}$$

for the translational control, and

$$\vec{m}_f = M_f \begin{bmatrix} \cos(\theta) \\ \sin(\theta) \\ 0 \end{bmatrix} \text{ and } \vec{m}_{cf} = M_{cf} \begin{bmatrix} \cos(\phi) \\ \sin(\phi) \\ 0 \end{bmatrix} \tag{8}$$

for the torsional control, where θ is the orientation angle of the torsional actuator's magnetic field.

The magnetic potential energy W_m is a nonlinear trigonometric expression. In order to analyse the dynamics of the coupling, the trigonometric terms of ϕ and ψ are replaced by their corresponding Taylor series expansions up to the second order around the equilibrium points $\phi = \psi = 0°$. The contribution from the magnetic interaction can then be concisely rewritten as:

$$W_m = -K_{m_1}\psi + K_{m_2}\phi + K_{m_3}\psi^2 + K_{m_4}\phi^2 + K_{m_5}\psi\phi + C, \tag{9}$$

with the coefficients:

$$K_{m_1} = 3\ell \left(\frac{M_{ct} M_t \mu_0}{2\pi (d_t + h)^4} + \frac{M_{cf} M_f \mu_0}{2\pi (d_f - h)^4} \cos(\theta) \right) \tag{10a}$$

$$K_{m_2} = \frac{M_{cf} M_f \mu_0}{4\pi (d_f - h)^4} (3R + d_f - h) \sin(\theta) \tag{10b}$$

$$K_{m_3} = 3\ell^2 \left(\frac{M_{ct} M_t \mu_0}{\pi (d_t + h)^5} - \frac{M_{cf} M_f \mu_0}{\pi (d_f - h)^5} \cos(\theta) \right) \tag{10c}$$

$$K_{m_4} = \frac{M_{cf} M_f \mu_0}{4\pi (d_f - h)^5} \left((d_f - h)^2 + 6R^2 + 6R d_f - 6Rh \right) \cos(\theta) \tag{10d}$$

$$- \frac{M_{ct} M_t \mu_0}{4\pi (d_t + h)^4} (3R + d_t + h)$$

$$K_{m_5} = 3\ell \left(\frac{M_{cf} M_f \mu_0}{4\pi (d_f - h)^5} (4R + d_f - h) \sin(\theta) \right) \tag{10e}$$

$$C = -\frac{M_{cf} M_f \mu_0}{2\pi (d_f - h)^3} \cos(\theta) + \frac{M_{ct} M_t \mu_0}{2\pi (d_t + h)^3}. \tag{10f}$$

The magnetic interaction couples the two degrees of freedom ψ and ϕ, through the coupling term K_{m_5} in the magnetic potential energy contribution (Equation (9)). Specifically, the external torques introduce magnetically induced stiffness-like terms, which interconnect the equations of motion through stiffness. The coupling is exclusively attributed to torsion, as K_{m_5} contains important parameters of the torsional control. After substitution of the relations above, the magnetic torques in Equation (1), are given by

$$T_t = +K_{m_1} - 2K_{m_3}\psi - K_{m_5}\phi \tag{11a}$$

$$T_f = -K_{m_2} - 2K_{m_4}\phi - K_{m_5}\psi. \tag{11b}$$

2.2 Control Strategy

The translational vibrations are controlled by adjusting the strength and polarity of the dipole M_t, while the orientation of the magnetic field of M_f is used to control the torsional rotation of the cylinder. In Equation (11b), the terms K_{m_1} and K_{m_2} serve as the controlled external forces acting on the system. The magnetic strength of the translational controller is governed by a proportional-derivative (PD) control equation, expressed as

$$M_t = K_p\, e + K_d\, \dot{e}, \text{ with } e = \xi - \ell\psi - h, \tag{12}$$

where the control gains are constant values with $K_p, K_d > 0$, and ξ represents the desired translational motion. The control rule for the torsional mode is defined by

$$\theta = \Delta\theta \tanh(\beta\dot{\phi}), \text{ with } \Delta\theta = \text{const.}, \tag{13}$$

where $\Delta\theta$ is the fluctuation step for the orientation of the magnetic actuator θ. Moreover, the parameter β controls the steepness of the transition between the

values around zero. As β approaches infinity, the control function converges to the standard sgn(..) function, while still providing a smooth and differentiable approximation.

2.3 Stability Requirements

To ensure a stable response, a condition concerning the magnetic strength M_t of the translational actuator must be satisfied. This condition directly affects the stability of the controlled dynamical system. Instability is undesirable as it results in an increasing amplitude of the response, which, within the proposed control scheme, can reduce the separation distance between the magnets. Such a reduction could potentially lead to "failure" of the control, as one of the pairs of magnetic dipoles may yield to the attracting forces and stick to each other.

Inspecting K_{m_1} as given by Equation (10a), two distinct torque actions are observed: one direct, exerted by the translational controller, and another indirect, generated by the horizontal components of the attractive force between the magnetic dipoles of the torsional controller. For an effective controlled response, the translational controller should counteract the additional torque around the pivot point induced by the torsional control. It is important to note that the translational control torque does not directly influence the motion in the xy-plane, except for the excitation amplitude at the pivot, as outlined in Equation (10b).

Therefore, it is suspected that the time trace of M_t will have a non-zero average value M_{t_0} around which the translational control variable will fluctuate with respect to the error and suspension motion. The amplitude of M_{t_0} arises from the main prerequisite for the stability of the system, neutralizing the torque generated by M_f in Equation (10b) , which yields

$$K_{m_2} = 0 \rightarrow \frac{M_{t_0}}{M_f} = -\cos(\theta)\frac{(d_t + h)^5}{(d_f - h)^5}. \tag{14}$$

3 Control of Translational and Torsional Vibrations

The control mode of interest pertains to the motion attenuation of the translational and torsional vibrations while subjected to an external excitation of its pivot and non-trivial initial conditions. The desired position of the suspended load is chosen $\psi = \phi = 0°$. The parameters of the controlled system are presented in Table 2.

Table 2. System parameters for the combined controlled vibrations.

M_f	M_{c_f} [A^2 m^4]	M_{c_t} [A m^2]	d_f [mm]	d_t [mm]	A_h [mm]	f_h [Hz]	ϕ_0 [°]	$\dot{\phi}_0$ [°/s]
5	-1	[30, 40, 50]	[30, 40, 50]	5	0.6	20	0	

For translational control, the PD controller's gains are determined heuristically to minimize error and enhance the controller's response. Thus, in this exemplary case, the proportional gain is set as $K_p = 3 \cdot 10^4\,\mathrm{A\,m}$ and the derivative gain as $K_d = 30\,\mathrm{A\,m\,s}$. Provided that the desired equilibrium of the torsional motion coincides with the intrinsic equilibrium of the system, the control rule given in Equation (13) becomes

$$\theta = \Delta\theta \tanh(\beta\dot{\phi}), \tag{15}$$

with the steepness coefficient $\beta = 1$ and the orientation alteration step $\Delta\theta = 5°$. Both controllers are activated at $t_s = 2$ s from the start of the simulation. This delay may lead to a more intricate transient response, aligning with the real application where vibrations would be present before the controllers are activated.

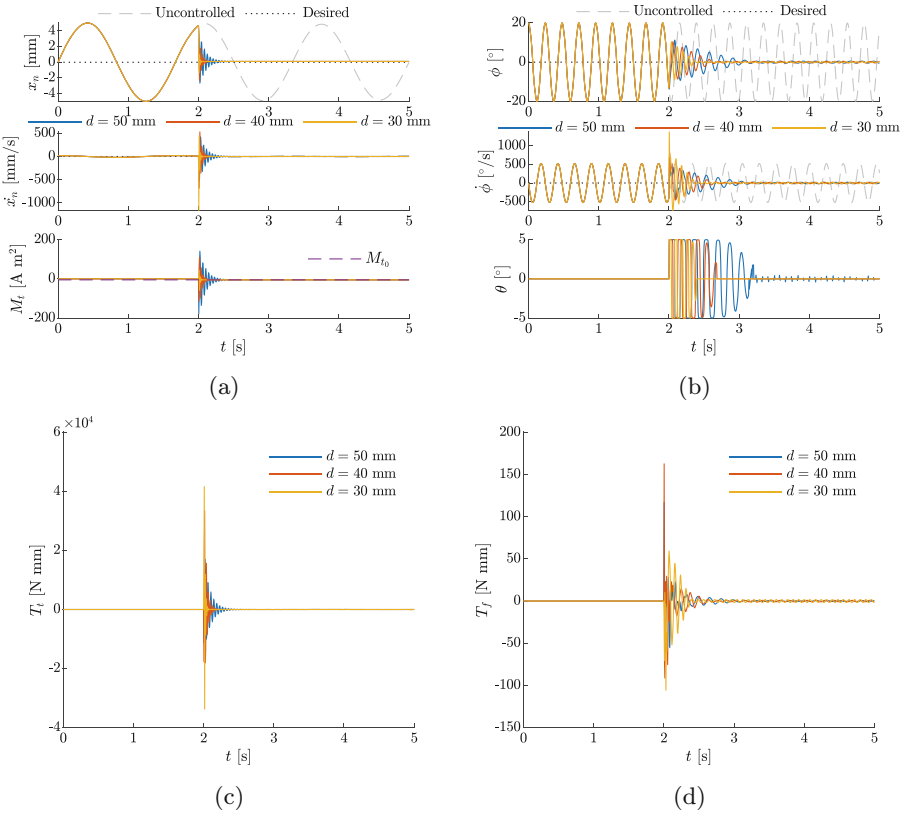

Fig. 2. Combined control efficiency metrics for motion attenuation. (a) Controlled response for translational vibrations. (b) Controlled response for torsional vibrations. (c) Effective actuation torque T_t for the translational control. (d) Effective actuation torque T_f for the torsional control.

Figure 2 displays the controlled (solid lines), desired (dotted line) and uncontrolled responses of the system (dashed line). More specifically, Fig. 2a demonstrates the effectiveness of the PD translational controller, achieving minimal steady-state error and a quick, smooth transient response, as indicated by the displacement and velocity time series. The different distances affect the strength of the magnetically induced damping, with $d = 30$ mm exhibiting the fastest dissipation. Notably, the control variable M_t, after successful translational control, settles at $M_t = -M_{t_0} = -M_f$, as predicted by Equation (14).

The controlled response of the torsional degree of freedom is depicted in Fig. 2b. In this case, the attenuation of motion is more gradual than in the translational response, displaying a damping mechanism similar to Coulomb friction, which is evident by the linear decay of the oscillations. To reduce the duration of the decay, an electromagnet strength M_f should be increased. Alternatively, the closer proximity of the two interacting dipoles yields similar favourable results (Fig. 2b).

On a general note, the different frequencies of the oscillation observed in the steady-state responses of the two degrees of freedom reflect the natural frequencies of the uncontrolled system.

In Figs. 2c and 2d, the two control torques exerted on the load are presented. The torque time series resembles the shape of the translational displacement and torsional angle time series. The highest amplitudes are observed for the translational torque T_t, whereas the torsional torque exhibits higher variation in the steady-state. Interestingly, the range of the translational torque is twice that of the torsional torque, highlighting the difference in control demands between the two degrees of freedom.

4 Conclusions

In the present paper, the combined control of two key degrees of freedom (translation and torsion) is analysed. The coupling presented due to the simultaneous action of the two actuators is reflected in the additional magnetically-induced stiffness terms in the equations of motion of the system. The mean amplitude of the translational control is dictated by the chosen amplitude of the torsional actuator dipole that is necessary to counteract the attraction forces exerted by the torsional dipole arrangement on the suspended load.

A combined control approach is evaluated for the mode of disturbance rejection for both translational and torsional motions. The controllers perform effectively, significantly reducing vibrations, with the translational response showing a rapid transition to the target steady state. The success of the combined control lies primarily in the precise motion control applied by the translational actuator, which determines the separation distance of the torsional dipoles, which is a critical factor in achieving efficient torsional control. The performance of the torsional controller can be further optimised by modifying the separation distance, magnetic strength, and orientation step of the external magnetic dipole.

In short, the contactless control succeeds in maintaining a desired fixed position while mitigating the motion of the magnetic pendulum imposed by external

pivot disturbance. The findings of this work underline the potential for the further advancement of this contactless motion control technique, and the eventual design of a more intricate multi-degree control algorithm for offshore applications.

References

1. Atzampou P, Meijers PC, Tsouvalas A, Metrikine AV (2024) Contactless control of suspended loads for offshore installations: proof of concept using magnetic interaction. Journal of Sound and Vibration 575:118246
2. Atzampou P, Meijers PC, Tsouvalas A, Metrikine AV (2025) Non-contact electromagnetic control of torsional vibrations of a rigid cylinder. Nonlinear Dynamics 113(3):2001–2016
3. Bassan M, De Marchi F, Marconi L, Pucacco G, Stanga R, Visco M (2013) Torsion pendulum revisited. Physics Letters A 377(25–27):1555–1562
4. Blackburn JA, Zhou-Jing Y, Vik S, Smith H, Nerenberg M (1987) Experimental study of chaos in a driven pendulum. Physica D: Nonlinear Phenomena 26(1–3):385–395
5. Jiang Z (2021) Installation of offshore wind turbines: a technical review. Renewable and Sustainable Energy Reviews 139:110576. https://doi.org/10.1016/J.RSER.2020.110576
6. Neupert J, Mahl T, Haessig B, Sawodny O, Schneider K (2008) A heave compensation approach for offshore cranes. In: Proceedings of the American Control Conference pp. 538–543. https://doi.org/10.1109/ACC.2008.4586547
7. O'Connor W, Habibi H (2013) Gantry crane control of a double-pendulum, distributed-mass load, using mechanical wave concepts. Mechanical Sciences 4:251–261. https://doi.org/10.5194/MS-4-251-2013
8. Ren Z, Jiang Z, Gao Z, Skjetne R (2018) Active tugger line force control for single blade installation. Wind Energy 21:1344–1358. https://doi.org/10.1002/WE.2258